Sensors and Actuators B 233 (2016) 479–485

Contents lists available at ScienceDirect

Sensors and Actuators B: Chemical

journal homepage: www.elsevier.com/locate/snb

A novel sensor for the detection of alkaline phosphatase activity based on the self-assembly of Eu^{3+}-doped oxide nanoparticles and heptamethine cyanine dye

Ben Hao Li [a], Ya Ling Zhang [a], Fan Shi Li [b], Wei Wang [a], Juan Liu [a], Min Liu [a], Yi Cui [a], Xia Bing Li [a], Bao Lin Li [a,*]

[a] Key Laboratory of Ministry of Education for Medicinal Resources and Natural Pharmaceutical Chemistry, and School of Chemistry & Chemical Engineering, Shaanxi Normal University, 710062 Xi'an, PR China
[b] Applied Chemical Institute, School of Chemical Engineering, Northwest University, 710069 Xi'an, PR China

ARTICLE INFO

Article history:
Received 3 December 2015
Received in revised form 13 April 2016
Accepted 18 April 2016
Available online 22 April 2016

Keywords:
Alkaline phosphatase sensor
$Y_{0.6}Eu_{0.4}VO_4$ nanoparticles
Heptamethine cyanine dye
Fluorescence assay
Inhibitor screening
Cell lysates

ABSTRACT

A non-fluorescent self-assemblage of $Y_{0.6}Eu_{0.4}VO_4$ nanoparticle (NP) and heptamethine cyanine dye bearing phosphate group p-Cy7-A, NP-p-Cy7-A, was the first constructed and used as an alkaline phosphatase (ALP) sensor. Herein, $Y_{0.6}Eu_{0.4}VO_4$ NP and new synthesized p-Cy7-A were employed respectively as donor and acceptor of Fluorescence Resonance Energy Transfer. With the help of phosphate group, p-Cy7-A as a dark quencher was captured on $Y_{0.6}Eu_{0.4}VO_4$ NP surface to form non-fluorescent NP-p-Cy7-A in situ. The disintegration of NP-p-Cy7-A was triggered by the removal of phosphate group in p-Cy7-A catalyzed by ALP, and released fluorescent $Y_{0.6}Eu_{0.4}VO_4$ NP. Thus NP-p-Cy7-A assemblage as a selective and sensitive sensor can very well responded to the amount and activity of ALP by measuring the fluorescent intensity at 620 nm (excited at 270 nm). This sensor can not only accurately measure the concentration of ALP (0.03–1.65 U/mL), but also be applied to detect the activity of ALP and screen its inhibitor by a simple mix-and-measure manner.

1. Introduction

Alkaline phosphatase (ALP) (EC 3.1.3.1), one of the most commonly hydrolase in mammalian tissues, particularly concentrated in liver, bile duct, kidney, bone and the placenta [1], is responsible for removing phosphate groups from various substrates, such as proteins, nucleotides, carbohydrates and alkaloids [2]. Its activity is often regarded as an important biomarker [3]. Abnormal level of ALP activity has been associated with a number of diseases including hepatitis, osteoporosis, prostatic cancer and bone tumor [4]. Therefore, ALP has become a useful tool in medical diagnosis, molecular biology laboratories [5] and the dairy industry as an indicator of successful pasteurization [6]. Considering the wide usage of ALP, many methods, such as electrochemistry [5,7], spectrophotometry [8], chemiluminescence [9], colorimetric [10] and fluorescence assays [11], have been successfully developed to assay the activity of ALP in various samples. Among them, fluorescent sensor with simple operation, high sensitivity and low background noise has attracted considerable attention [12]. However, these reported methods have some limitations such as complicated sensing mechanism, short fluorescence lifetime, short emission wavelength [11][11e], or specialized bioconjugation step [13]. Therefore, it is desirable to develop a convenient and sensitive method for the monitoring of ALP activity in real-time.

Recently, lanthanide (Ln) complexes and nanoparticles (NPs) have shown a great prospect in various applications, such as cancer diagnosis [14], the detection of protein kinase activity [15] and the monitoring of hydrogel degradation [16] etc. This is based on the excellent chemical and optical properties of lanthanide materials, including low toxicity, long fluorescence lifetime in the millisecond range, large Stokes shift, narrow emission spectra, as well as high resistance to blinking, photobleaching and photochemical degradation [17]. Compared to Ln^{3+} complexes, NPs do not need the complicated process for the preparation of ligand. Meanwhile, one lanthanide NP contains multi-lanthanide atoms. Thus, one NP can absorb multi-photons, which results in the excitation of multi-lanthanide atoms at the same time. This feature makes lanthanide NPs have the potential to dramatically improve the sensitivity of fluorescence assay. Considering that the outstanding property of lanthanide NPs, we focused on developing a novel turn-on lan-

* Corresponding author.
E-mail address: baolinli@snnu.edu.cn (B.L. Li).

http://dx.doi.org/10.1016/j.snb.2016.04.102
0925-4005/

thanide NPs-based sensor for the detection of ALP activity and its inhibitor screening. This paper presents our recent results.

2. Experimental

2.1. Synthesis materials and instruments

All reagents were of analytical grade and were used directly as obtained commercially unless otherwise stated. Alkaline phosphatase from bovine intestinal mucosa (4500U/mg) were purchased from Shanghai Yuanye Bio-Technolgy Co., Ltd. β-Glucosidase, RNase A, lysozyme, trypsin, Penicillin-Streptomycin (P/S), L-glutamate, Tris, Dithiothreitol (DTT), Levamisole, $Y(NO_3)_3{\cdot}6H_2O$, $Eu(NO_3)_3{\cdot}6H_2O$ and $Na_3VO_4{\cdot}12H_2O$ were purchased from Sigma-Aldrich. Human cervical carcinoma Hela cells were kindly supplied by Chia Tai Tian Qing Pharmaceutical Group Co., Ltd. Dulbecco's Modified Eagle's Medium (DMEM), Fetal Bovine Serum (FBS) were purchased from Gibco. One step animal cell active protein extraction kit was purchased from Sangon Biotech. BCA protein assay kit was purchased from Beijing Biodragon Immunorechnologies Co., Ltd.

Absorption and emission spectra were collected by using a Shimadzu 1750 UV–vis spectrometer and a Hitachi F-7000 fluorescence spectrometer, respectively. ^{1}HNMR, ^{13}CNMR and ^{31}P NMR spectra were measured with a Bruker AV 400 or 600 NMR spectrometer. The high-resolution mass spectra (HRMS) were measured in ESI negative mode using Bruker maxis UHR-TOF mass spectrometer. The FTIR spectra were acquired on a Fourier transform infrared spectrometer (Vertex 70 v, Bruker, Germany). The hydrodynamic radius of nanoparticle was investigated through dynamic light scattering (DLS) techniques. The experiments were performed by using a Malven Autosizer 4700 DLS spectrometer with scattering angle of 90°. Transmission electron microscopy (TEM) measurements were conducted on a Philips CM 120 electron microscope at an acceleration voltage of 100 kV. The samples for TEM observations were prepared by evaporating 10 μL related solution onto a carbon-coated film supported on a 3 mm, 300 mesh copper grid.

2.2. Preparation of $Y_{0.6}Eu_{0.4}VO_4$ NPs, p-Cy7-A, p-Cy7.5-A and Cy7-A

$Y_{0.6}Eu_{0.4}VO_4$ NPs, p-Cy7-A, p-Cy7.5-A and Cy7-A were prepared according to the detailed description in the supporting information.

2.3. Sample preparation

Stock solution of levamisole was prepared in buffer A (20 mM Tris-HCl, 2 mM $MgCl_2$, 2 mM DTT, pH 8.0). Stock solutions of p-Cy7-A and p-Cy7.5-A (6.0×10^{-4} M) were prepared in CH_3OH. ALP was dissolved in buffer A to form the ALP stock solution and stored at −30 °C. The colloidal solutions of $Y_{0.6}Eu_{0.4}VO_4$ NPs were obtained by dispersing freshly prepared NPs to Tris-HCl buffer (20 mM, pH 8.0) or buffer A with the help of ultrasonic wave.

2.4. The formation of NP-p-Cy7-A sensor

A series of test solution of NP-p-Cy7-A assemblage were obtained by adding different amount of p-Cy7-A stock solution to the NPs colloidal solution in buffer A. In these test solutions, the final concentration of NPs was controlled at 6 mM. The obtained test solutions were shaken and equilibrated for 3 min before the fluorescent measurements. Fluorescence measurement conditions were controlled by 5 nm (ex slit), 5 nm (em slit). The excitation wavelength was selected at 270 nm.

2.5. Cell culture and the collection of cell lysate

Hela Cells were incubated in DMEM supplemented with 10% (v/v) FBS, 1% P/S and 1% L-glutamate in a humidified incubator containing 5% CO_2 at 37 °C. When 90% confluence was reached, the cultured cells were harvested and lysed with the one step animal cell active protein extraction kit. Briefly, the culture medium was removed, and the cells were washed 3 times with PBS, and then lysed with the lysis buffer on ice for 30 min, the supernatant was collected by centrifugation at $1000 \times g$ for 10 min, and was stored at −80 °C until use [11,15][11a,15]. The protein concentration in the supernatant was determined by using a BCA protein assay kit.

2.6. The fluorescent sensor for detection of ALP and other enzymes by mix-and-measure

The ALP, the lysate of Hela cells or other enzymes were added to buffer A containing the aforementioned NP-p-Cy7-A assemblage at 30 °C. After stirring for 30 min, the fluorescent intensity of the mixture was directly measured at 620 nm (λ_{ex} = 270 nm) by using Hitachi F-7000 fluorescence spectrometer without any further treatment. In these test solutions, the total volume was 2 mL, the final concentrations of NPs and p-Cy7-A were 6 mM and 6 μM, respectively. Fluorescent measurement conditions were controlled by 5 nm (ex slit), 5 nm (em slit).

To confirm the application of the sensor in the screening of ALP inhibitor, the inhibition effect of levamisole on ALP activity was tested. The stock solution of levamisole was added into NPs colloidal solution in buffer A containing ALP (2.50 U/mL) or the lysate of Hela cells (0.35 mg/mL). After mixing for 20 min, 20 μL of p-Cy7-A stock solution was added and mixed for 30 min. The fluorescent intensity of mixture were monitored by fluorescence spectrometer at 620 nm (λ_{ex} = 270 nm). In these test solutions, the total volume was 2 mL, the final concentrations of NPs and p-Cy7-A were 6 mM and 6 μM, respectively. And the final concentrations of levamisole were controlled from 0 to 4 mM, respectively. Fluorescence measurement conditions were controlled by 5 nm (ex slit), 5 nm (em slit).

2.7. The calculation of kinetic parameters of ALP activity

The kinetic parameters of ALP were determined with different p-Cy7-A concentrations from 0 ~ 6 μM. Lineweaver–Burk plot was obtained using double reciprocal data of initial rate v vs p-Cy7-A concentrations $[S]_0$ as in Eq. (1)

$$1/v = K_m/(V_{max}[S]_0) + 1/V_{max} \quad (1)$$

where v is the initial rate and acquired from the range of the plots in Fig. 3(b) using the beginning 3 points; $[S]_0$ is the initial concentration of p-Cy7-A; K_m is the Michaelis constant; V_{max} is the maximal rate.

The original fluorescence data applied in this calculation is shown in Fig. S1 (ESI†).

2.8. The calculation of detecting limit of ALP

Detecting limit (DL) is obtained using the following equation:

$$DL = k \times sb/s$$

where k = 3, sb is the standard derivation of the blank solution and s is the slope of the calibration curve.

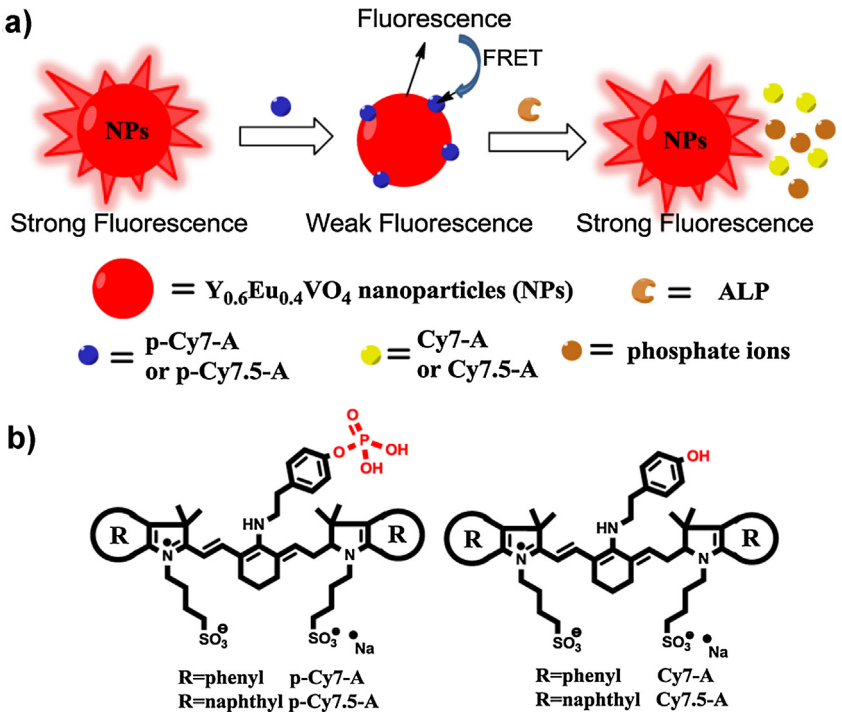

Scheme 1. (a) The illustration of ALP sensor based on the self-assembly of NPs and p-Cy7-A/p-Cy7.5-A. (b) The chemical structures of p-Cy7-A/p-Cy7.5-A and Cy7-A/Cy7.5-A.

2.9. The calculation of concentrations of p-Cy7-A and Cy7-A (hydrolyzed from p-Cy7-A)

To accurately evaluate the kinetics of the enzymes, the concentrations of the unhydrolyzed substrate p-Cy7-A at different time were calculated by fluorescence intensity data based on Eq. (2):

$$[S]_t = [S]_0[(I_0/I_t - 1)/(I_0/I_q - 1)] \quad (2)$$

where $[S]_t$ is the concentration of p-Cy7-A at time t; $[S]_o$ is the initial concentration of p-Cy7-A; I_q is the emission intensity of the mixture of NPs (6 mM) and p-Cy7-A in the different initial concentration (0 ~ 6 μM) in buffer A; I_0 is the emission intensity of the mixture of NPs (6 mM) and ALP (2.5 U/mL) in buffer A and I_t is the emission intensity of the mixture of NPs (6 mM) and ALP (2.5 U/mL) under the different initial concentration of p-Cy7-A (0 ~ 6 μM) in buffer A at reaction time t.

The concentrations of Cy7-A (hydrolyzed from p-Cy7-A) at different time were derived from Eq. (3)

$$[Cy7\text{-}A]_t = [S]_0 - [S]_t \quad (3)$$

where $[S]_0$ is the initial concentration of p-Cy7-A in buffer A and $[S]_t$ is the concentration of p-Cy7-A at reaction time t.

3. Results and discussion

3.1. Design, synthesis and sensing mechanism

To obtain a high-efficiency and low-cost ALP sensor, we designed a new non-fluorescent Fluorescence Resonance Energy Transfer (FRET) system. The simple mechanism is illustrated as shown in Scheme 1a. Eu^{3+} doped oxide NPs $Y_{0.6}Eu_{0.4}VO_4$ was chosen as a fluorescent donor. And either of heptamethine cyanine dyes with phosphate group, p-Cy7-A or p-Cy7.5-A (Scheme 1b), was selected as dark quencher. These two components were coupled to the donor-acceptor pair of FRET. The previous literatures have demonstrated that Ln^{3+} possesses high binding capacity to phosphate group [18]. Thus non-fluorescent self-assemblages based on FRET, $Y_{0.6}Eu_{0.4}VO_4$-NP-p-Cy7-A (NP-p-Cy7-A) or $Y_{0.6}Eu_{0.4}VO_4$-NP-p-Cy7.5-A, should be able to form through Eu^{3+}-doped oxide NP capturing p-Cy7-A or p-Cy7.5-A on NP surface with the help of phosphate group. The disintegrations of assemblages may be triggered by the removal of phosphate group in p-Cy7-A or p-Cy7.5-A catalyzed by ALP, and release fluorescent $Y_{0.6}Eu_{0.4}VO_4$ NP. Meanwhile p-Cy7-A or p-Cy7.5-A will be transformed to Cy7-A or Cy7.5-A. In the case, this turn-on fluorescence system should be able to well respond to the activity and amount of ALP.

Casanova et al. had used a very simple precipitation reaction of $Y(NO_3)_3$, $Eu(NO_3)_3$ and Na_3VO_4 to successfully prepare $Y_{0.6}Eu_{0.4}VO_4$ NPs [19]. To obtain a fluorescent donor, the $Y_{0.6}Eu_{0.4}VO_4$ NPs were prepared by using Casanova's method straightforward. The diameter of the obtained NPs was measured to be 56.8 nm by DLS techniques, which is consistent with the result from TEM (Fig. 1a and 1d). A 6 mM colloidal solution of $Y_{0.6}Eu_{0.4}VO_4$ NPs was prepared by dispersing the obtained NPs freshly to Tris-HCl buffer (20 mM, pH 8.0) with the help of ultrasonic wave. The colloidal solution was still stable even after standing for 6 months at 4 °C. When the colloidal solution was radiated with 270 nm UV light, the characteristic emission peaks of Eu^{3+} were exhibited at 596 ($^5D_0 \rightarrow {}^7F_1$), 620 ($^5D_0 \rightarrow {}^7F_1$), 652 ($^5D_0 \rightarrow {}^7F_1$) and 700 ($^5D_0 \rightarrow {}^7F_1$) nm (Fig. S2, ESI†). In all emission peaks, the peak at 620 nm appeared maximal emission intensity as shown in Fig. 2a. These fluorescent emissions owe to that the absorption of UV photons by the VO_4^{3-} group inside the host matrix is followed by nonradiative transfer to the Eu^{3+}, and the latter come back to the ground state through a radiative transition [20].

Herein, dark quencher as an acceptor of FRET, its absorption spectrum should be overlap with the emission spectrum of donor, meanwhile it should possess high extinction coefficient. Cyanine dye is a good candidate for such studies. Peng et al. synthesized a series of cyanine dyes with absorption wavelengths in the near IR region of about 650–900 nm, and the dyes are essentially non-fluorescent. These dyes were used as near IR quenchers to label antibodies and peptides for biological assays [21]. Kiyose et al. prepared several amino-heptamethine dyes through the

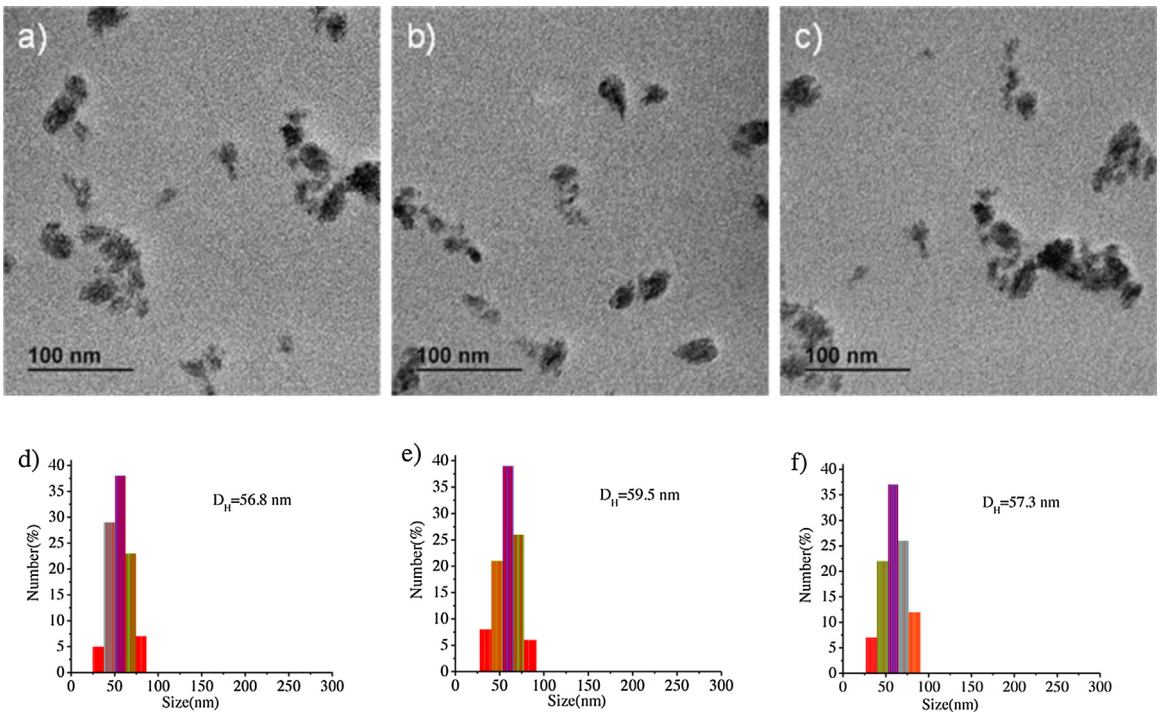

Fig. 1. TEM images of (a) NPs; (b) the mixture of NPs and p-Cy7-A; (c) the mixture of NPs, p-Cy7-A and ALP. DLS of (d) NPs; (e) the mixture NPs and p-Cy7-A; (f) the mixture of NPs, p-Cy7-A and ALP. [NPs] = 6 mM, [p-Cy7-A] = 6 μM, [ALP] = 2.50 U/mL.

nucleophilic substitution of Cl in IR-786, and they found an obvious change in the wavelength of the absorption maximum from 774 nm of IR-786 to about 626 nm of aminocyanine dyes [22]. We were inspired by these studies and would like to obtain a water-soluble amino-heptamethine dyes which can be captured by $Y_{0.6}Eu_{0.4}VO_4$ NPs with the help of phosphate group. Through the nucleophilic substitutions of tyramine-*O*-phosphate and IR-786 analogues (IR-783 or IR-820), two novel amino-heptamethine dyes bearing phosphate group, p-Cy7-A and p-Cy7.5-A, were successfully synthesized (Scheme S1, ESI†), respectively. Their wavelengths of the maximum absorption are at 620 and 651 nm with high extinction coefficients (p-Cy7-A: $\varepsilon = 3.2 \times 10^4\ M^{-1}\ cm^{-1}$, p-Cy7.5-A: $\varepsilon = 3.6 \times 10^4\ M^{-1}\ cm^{-1}$) in buffer A (20 mM Tris-HCl, 2 mM $MgCl_2$, 2 mM DTT, pH 8.0). However, they exhibited very low intensity of the maximum emission at 730 and 735 nm ($\Phi_F < 0.001$), when they were excited at 620 and 650 nm, respectively (Fig. S3–4, ESI†). This non-fluorescence characteristic of the amino-cyanine dyes may due to a nonradiative relaxation by ICT-TICT rotary decay model [23]. We also observed that the absorption spectrum of p-Cy7-A was more excellent overlap with the emission spectrum of $Y_{0.6}Eu_{0.4}VO_4$ NPs than that of p-Cy7.5-A as shown in Fig. 2a. This important feature suggested that p-Cy7-A was a more efficient quencher than p-Cy7.5-A in designed FRET system. Thus, p-Cy7-A was selected for the following investigation.

3.2. The formation of non-fluorescent self-assemblage NP-p-Cy7-A

As expected, when p-Cy7-A was added to the solution of 6 mM $Y_{0.6}Eu_{0.4}VO_4$ NPs in buffer A, the fluorescent intensity of NPs appeared obviously decay at 596, 620, 652 and 700 nm after stirring for 3 min (Fig. 2b, S6–8, ESI†). With the increasing of the concentration of p-Cy7-A from 0 to 6.6 μM, the fluorescent intensity of NPs was reduced gradually. When the concentration of p-Cy7-A was

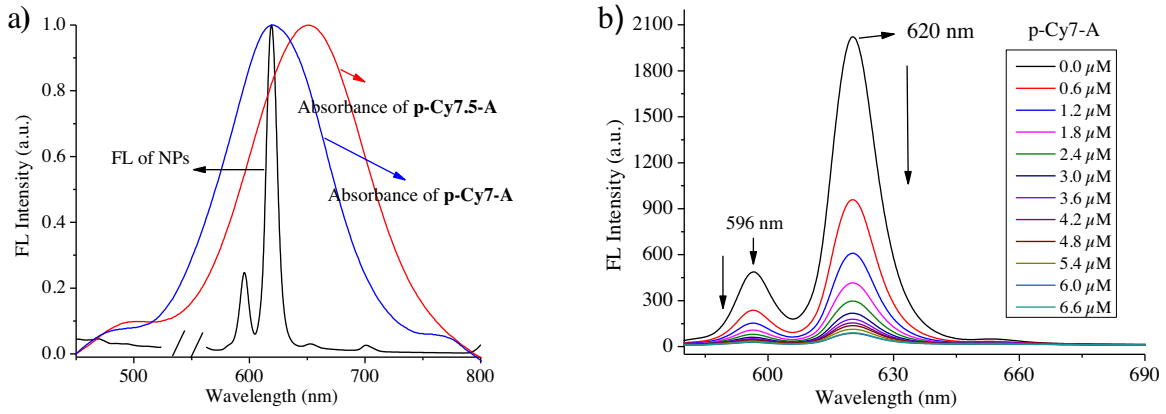

Fig. 2. (a) The emission (black line) and UV-Vis (blue and red line) spectra of NPs, p-Cy7-A and p-Cy7.5-A in buffer A; (b) The fluorescence spectra of NPs (6 mM) in the presence of different concentration of p-Cy7-A (0-6.6 μM) in buffer A (λ_{ex} = 270 nm). (For interpretation of the references to colour in this figure legend, the reader is referred to the web version of this article.)

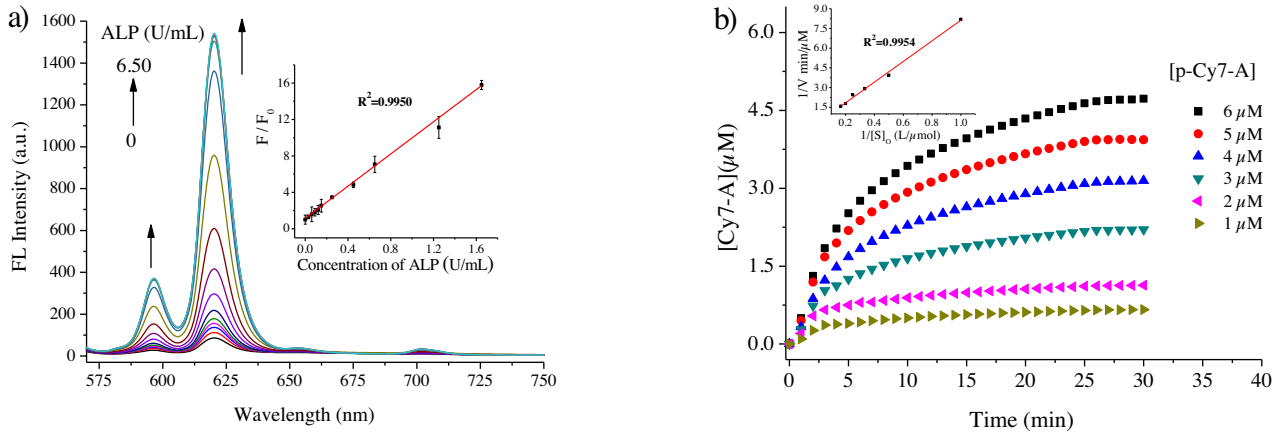

Fig. 3. (a) The fluorescent change of the assemblage NP-p-Cy7-A (the concentrations of NPs and p-Cy7-A in 6 mM and 6 μM, respectively) in buffer A with the increasing of the concentration of ALP (λ_{ex} = 270 nm) (inset: the linear relationship of fluorescence intensity ratio (F/F_0) to the concentration of ALP, where F and F_0 stand for the fluorescence intensity at 620 nm (λ_{ex} = 270 nm) in the presence and absence of ALP); (b) The concentration change of hydrolysis product Cy7-A with the increasing of the incubation time of ALP (2.5 U/mL) and NPs (6 mM) under the different initial concentration of p-Cy7-A (Inset: The Lineweaver–Burk plot for determination of K_m).

6.0 μM, the fluorescent intensity of NPs at 620 nm was reduced to the weakest. This means that the fluorescence of NPs at 620 nm can be almost completely quenched by p-Cy7-A at the concentration ratio of 1000:1 (NPs: p-Cy7-A). The results indicated definitely that FRET has occurred between NP and p-Cy7-A because of the self-assemblage formation of NP-p-Cy7-A, resulting from very close proximity of p-Cy7-A and NP. Meanwhile, we would like to investigate that if the aggregation of NPs could occur with addition of p-Cy7-A. Thus the size of NPs was determined by using TEM and DLS (Fig. 1b and 1e). The result indicated the diameter of NPs was 59.5 nm, and the aggregation did not happen. In contrast, by using Cy7-A instead of p-Cy7-A under the same condition, the change of the fluorescent intensity of NPs was seldom observed. Even if high concentration (50 μM) of Cy7-A was mixed with 6 mM NPs for longer duration of stirring (65 min), no signal change was observed (Fig. S9–10, ESI†). It suggested that the phosphate group in p-Cy7-A is very important for pulling p-Cy7-A to the surface of NPs. Ln ions are hard Lewis acids and can bind with negatively charged phosphate groups rather than sulphonic groups [24]. The trivalent Ln ion has abundant f-orbitals which expand the coordination site to bind six to twelve ligands to one single metal ion [25]. These facts give us a clear indication that Eu ions in the NPs serve as a powerful captor for recognizing phosphorylated heptamethine cyanine dye.

3.3. ALP assay based on the fluorescence recovery

The response of non-fluorescent self-assemblage NP-p-Cy7-A to ALP was observed from the fluorescent recovery of the NPs, when ALP was added to the solution of NP-p-Cy7-A formed in situ by mixing NPs (6 mM) and p-Cy7-A (6 μM) in buffer A (Fig. 3a, S11, ESI†). If the concentration of ALP was increased from 0 to 6.5 U/mL at 37 °C for the reaction of 30 min, the fluorescent intensity of the system at 620 nm (λ_{ex} = 270 nm) was increased 17.8-fold compared to that of the absence of ALP. The result indicated the disintegration of NP-p-Cy7-A self-assemblage led to the break of FRET system resulting from the removal of phosphate group of p-Cy7-A, the release of fluorescent $Y_{0.6}Eu_{0.4}VO_4$ NP, and the generation of Cy7-A (Φ_F < 0.001, Fig. S5 ESI†) in the presence of ALP. This was proved by HRMS analysis of the mixture of enzymatic reaction. As shown in Fig. S12 (ESI†), the peaks at *m/z* 826.3578 and 412.6750 are assigned to the hydrolysis product Cy7-A in −1 ($[Cy7\text{-}A]^-$ calcd = 826.3565) and −2 valence state ($[Cy7\text{-}A]^{2-}$ calcd = 412.6746), respectively. This result firmly supported that the p-Cy7-A was hydrolyzed to Cy7-A under the catalysis of ALP. Similarly, the aggregation of the assemblage NP-p-Cy7-A was not also observed when ALP was added to the solution of the assemblage. This result was deduced from the relevant experiments of TEM and DLS (Fig. 1c and 1f).

In order to apply the non-fluorescent self-assemblage NP-p-Cy7-A as an ALP sensor, the enzymatic hydrolysis of p-Cy7-A in FRET system was further optimized. As shown in Fig. S11, when the concentration of ALP was in 2.5 U/mL, the fluorescent intensity of the system increased to the maximum value. After that, the fluorescent intensity no longer increased. We also found that the fluorescence intensity of 620 nm gradually increased with the increasing of incubation time of the assemblage with ALP of 2.5 U/mL and it then reached maximum after incubation for 30 min (Fig. S13–14, ESI†). Meanwhile, the effect of the concentrations on sensitivity was investigated under obtained condition. When the concentration ratio of the NPs and p-Cy-A was constant in 1000:1, with increasing the concentration of the NPs from 1 to 8 mM in buffer A, the fluorescence intensity ratio (F/F_0) at 620 nm in the presence and absence of ALP (2.5 U/mL) exhibited an increasing trend (Fig. S15, ESI†). High F/F_0 should lead to a higher detection sensitivity. This result indicated that the concentration of the NPs from 6 to 8 mM is suitable to detect ALP. Herein the NPs concentration of 6 mM along with p-Cy-A concentration of 6 μM were selected for the formation of assemblage. So the incubation of the mixture of the assemblage and ALP for 30 min at 37 °C was selected to investigate the viability of the sensor for the fluorescent detection of ALP. As shown in Fig. 3a (inset), there was a good linear relationship between the fluorescence ratios F/F_0 (F and F_0 denote the fluorescent intensity at 620 nm in the presence or the absence of ALP) and the ALP concentrations from 0.03 to 1.65 U/mL (R^2 = 0.9950). The result indicated that the sensor generated in situ can be applied to accurately determine ALP with the detection limit as low as 8.45 mU/mL. Compared with previous reported ALP sensor (Table S1, ESI†), besides the similar fit range of concentration and the detection limit, the assemblage NP-p-Cy7-A supplies a simpler method for the determination of ALP.

In addition, we determined the kinetic parameters for the hydrolysis of p-Cy7-A catalyzed by ALP under different initial p-Cy7-A concentrations. As shown in Fig. 3b, the results from Lineweaver–Burk analysis, K_m = 28.3 μM, k_{cat} = 0.18 s^{-1} and $k_{cat}/K_m = 6.3 \times 10^3\ M^{-1}s^{-1}$, agreed with the data reported in the literature [11][11a].

To demonstrate that the assemblage NP-p-Cy7-A is a selective sensor of ALP, a control experiment with other enzymes, such as β-glucosidase, RNase A, lysozyme, and trypsin, was performed under the same conditions. As shown in Fig. S16, a 17.3-fold fluorescence enhancement at 620 nm was only observed when ALP

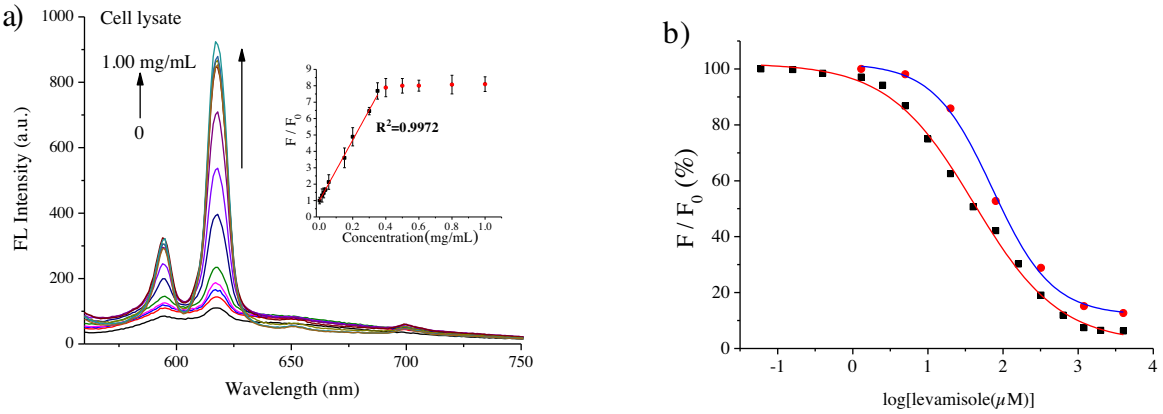

Fig. 4. (a) The fluorescent change of the mixture of NPs (6 mM) and p-Cy7-A (6 μM) in buffer A with increasing the concentration of cell lysate (λ_{ex} = 270 nm) (inset: the linear relationship of fluorescence intensity ratio (F/F_0) to the concentration of cell lysate, where F and F_0 stand for the fluorescence intensity at 620 nm in the presence and absence of cell lysate); (b) Inhibition effect of levamisole on ALP (red line) and cell lysate (blue line) (where F and F_0 stand for the fluorescence intensity at 620 nm in the presence and absence of ALP or cell lysate). (For interpretation of the references to colour in this figure legend, the reader is referred to the web version of this article.)

(2.50 U/mL) was added to the solution of the assemblage NP-p-Cy-A. The result demonstrated that the assemblage NP-p-Cy7-A is an excellent selective sensor for ALP.

3.4. Detection of ALP activity in cell lysates

To demonstrate the feasibility of the sensor for monitoring the ALP activity in real biological samples, an ALP assay in cell lysates was investigated. Herein, Hela cell lysate was tested as a biological sample because Hela human cervical carcinoma cell line is known to express endogenous ALP [11][11a]. As shown in Fig. 4a, instead of ALP with the lysate of Hela cell, the fluorescence intensity at 596 and 620 nm for the mixture of NPs (6 mM) and p-Cy7-A (6 μM) in buffer A were enhanced with the increasing of the amount of cell lysate. Monitoring at 620 nm (λ_{ex} = 270 nm), the fluorescence intensity of system showed a linear increasing relationship with the concentration of the cell lysate in 0 ~ 0.35 mg/mL range and then reached a plateau after the concentration of cell lysate more than 0.4 mg/mL (inset in Fig. 4a). The result indicated the NP-p-Cy7-A sensor formed in situ is very well respond to ALP in real biological samples, and able to detect the activity of ALP in real-time through a simple mix-and-measure manner.

3.5. Application of the sensor in the screening of ALP inhibitor

To confirm the potential of the sensor in the screening of ALP inhibitor, levamisole, a well-known ALP inhibitor, was used to check the response of the sensor to ALP activity. In optimized condition, the inhibition of ALP activity was carried out by adding a series amount of levamisole to the mixture of $Y_{0.6}Eu_{0.4}VO_4$ NPs (6 mM) and ALP (2.50 U/mL) in buffer A. Then, to the mixture containing ALP inhibitor, p-Cy7-A was added. After 30 min, the fluorescence intensity of the system was measured at 620 nm (λ_{ex} = 270 nm). It was found the fluorescence intensity responded well to the formation of NP-p-Cy7-A and the amount of levamisole (see Fig. S17 ESI†). Indeed, with the increase of the concentration of levamisole, the amount of the formed NP-p-Cy7-A was raised due to the hydrolysis of p-Cy7-A was blocked in the presence of low active ALP. This led to the system exhibited lower fluorescence intensity at 620 nm. As shown in Fig. 4b, the IC_{50} of levamisole is 39.8 μM calculated by using the sigmoidal fit. These results firmly supported that this sensor can be used to investigate the inhibition effect of levamisole on ALP activity [11][11a]. Similar result, 75.1 μM of IC_{50} for levamisole, was obtained from replacing ALP with the lysates of Hela cells (0.35 mg/mL) (see Fig. 4b, S18, ESI†). These results proved that NP-p-Cy7-A sensor can be utilized to detect the inhibition effect of levamisole on ALP in real biological samples such as cell lysate, and to screen ALP inhibitor.

4. Conclusion

In summary, a high-efficiency ALP sensor, based on the FRET of $Y_{0.6}Eu_{0.4}VO_4$ nanoparticles with p-Cy7-A, was demonstrated for the highly selective and sensitive detection of alkaline phosphatase in real-time and the screening of ALP inhibitor. This ALP sensor is formed in situ as a non-fluorescent self-assemblage by mixing $Y_{0.6}Eu_{0.4}VO_4$ nanoparticles with p-Cy7-A. The formed sensor can decompose to fluorescent $Y_{0.6}Eu_{0.4}VO_4$ nanoparticles under the catalysis of ALP. On the other hand, the amount of the formed sensor can be reduced in the test mixture in the presence of ALP because of the hydrolysis of p-Cy7-A. However, the amount of sensor can be raised in the test mixture in the presence of both ALP and its inhibitor. All these processes can be traced by recording the fluorescent changes. This gives us a simple mix-and-measure manner to determine ALP by using the developed sensor. To our best knowledge, this is the first ALP sensor based on the FRET of lanthanide-doped oxide NPs and near-infrared cyanine dyes bearing phosphate group. Because of the longer fluorescence emission wavelength, this ALP sensor can vastly eliminate auto-fluorescent background of biological samples. The application of the fluorescence technique, based on straight forward mix-and-measure solution chemistry, holds the promise for simple, rapid and cheap biosensors that may be applied in various biological systems. Further work on the application of disease diagnosis is in progress.

Acknowledgments

This work was financially supported by the National Natural Science Foundation of China (No.21272144).

Appendix A. Supplementary data

Supplementary data associated with this article can be found, in the online version, at http://dx.doi.org/10.1016/j.snb.2016.04.102.

References

[1] N.J. Fernandez, B.A. Kidney, Alkaline phosphatase: beyond the liver, Vet. Clin. Pathol. 36 (2007) 223–233.

[2] M. Syakalima, M. Takiguchi, J. Yasuda, A. Hashimoto, The canine alkaline phosphatases: a review of the isoenzymes in serum, analytical methods and their diagnostic application, J. Vet. Res. 46 (1998) 3–11.
[3] J.E. Coleman, Structure and mechanism of alkaline phosphatase, Annu. Rev. Biophys. Biomol. Struct. 21 (1992) 441–483.
[4] R.E. Gyurcsanyi, A. Bereczki, G. Nagy, M.R. Neuman, E. Lindner, Amperometric microcells for alkaline phosphatase assay, Analyst 127 (2002) 235–240.
[5] A.F. Pike, N.I. Kramer, B.J. Blaauboer, W. Seinen, R. Brands, A novel hypothesis for an alkaline phosphatase 'rescue' mechanism in the hepatic acute phase immune response, Biochim. Biophys. Acta Mol. Basis Dis. 1832 (2013) 2044–2056.
[6] S.M. Albillos, R. Reddy, R. Salter, Evaluation of alkaline phosphatase detection in dairy products using a modified rapid chemiluminescent method and official methods, J. Food. Prot. 74 (2011) 1144–1154.
[7] P. Miao, L. Ning, X. Li, Y. Shu, G. Li, An electrochemical alkaline phosphatase biosensor fabricated with two DNA probes coupled with λ exonuclease, Biosens. Bioelectron. 27 (2011) 178–182.
[8] A. Bianchi, E. Giachetti, P. Vanni, A continuous spectrophotometric assay for alkaline phosphatase with glycerophosphate as substrate, J. Biochem. Biophys. Methods 28 (1994) 35–41.
[9] R.S. Salter, J. Fitchen, Evaluation of a chemiluminescence method for measuring alkaline phosphatase activity in whole milk of multiple species and bovine dairy drinks: interlaboratory study, JAOAC Int. 89 (2006) 1061–1070.
[10] Y. Choi, N.-H. Ho, C.-H. Tung, Sensing phosphatase activity by using gold nanoparticles, Angew. Chem. Int. Ed. 46 (2007) 707–709.
[11] (a) T.I. Kim, H. Kim, Y. Choi, Y. Kim, A fluorescent turn-on probe for the detection of alkaline phosphatase activity in living cells, Chem. Commun. 47 (2011) 9825–9827;
(b) E.K. Lim, J.O. Keem, H.S. Yun, J. Jung, B.H. Chung, Smart nanoprobes for the detection of alkaline phosphatase activity during osteoblast differentiation, Chem. Commun. 51 (2015) 3270–3272;
(c) Y. Zhu, G. Wang, H. Jiang, L. Chen, X. Zhang, One-step ultrasonic synthesis of graphene quantum dots with high quantum yield and their application in sensing alkaline phosphatase, Chem. Commun. 51 (2015) 948–951;
(d) Y. Obayashi, R. Iino, H. Noji, A single-molecule digital enzyme assay using alkaline phosphatase with a cumarin-based fluorogenic substrate, Analyst 140 (2015) 5065–5073;
(e) Z.S. Qian, L.J. Chai, Y.Y. Huang, C. Tang, J.S. Jia, J.R. Chen, et al., A real-time fluorescent assay for the detection of alkaline phosphatase activity based on carbon quantum dots, Biosens. Bioelectron. 68 (2015) 675–680.
[12] (a) T. Anand, G. Sivaraman, P. Anandh, D. Chellappa, S. Govindarajan, Colorimetric and turn-on fluorescence detection of Ag(I) ion, Tetrahedron Lett. 55 (2014) 671–675;
(b) O. Sunnapu, N.G. Kotla, B. Maddiboyina, S. Singaravadivel, G. Sivaraman, A rhodamine based "turn-on" fluorescent probe for Pb(ii) and live cell imaging, RSC Adv. 6 (2016) 656–660;
(c) G. Sivaraman, D. Chellappa, Rhodamine based sensor for naked-eye detection and live cell imaging of fluoride ions, J. Mater. Chem. B 1 (2013) 5768–5772;
(d) K.M. Vengaian, C.D. Britto, K. Sekar, G. Sivaraman, S. Singaravadivel, Fluorescence "on-off-on" chemosensor for selective detection of Hg^{2+} and S^{2-}: application to bioimaging in living cells, RSC Adv. 6 (2016) 7668–7673;
(e) G. Sivaraman, T. Anand, D. Chellappa, Turn-on fluorescent chemosensor for Zn(ii) via ring opening of rhodamine spirolactam and their live cell imaging, Analyst 137 (2012) 5881–5884;
(f) G. Sivaraman, B. Vidya, D. Chellappa, RSC Adv. 4 (2014) 30828–30831.
[13] S. Liu, S. Pang, W. Na, X. Su, Near-infrared fluorescence probe for the determination of alkaline phosphatase, Biosens. Bioelectron. 55 (2014) 249–254.
[14] L. Zhou, R. Wang, C. Yao, X. Li, C. Wang, X. Zhang, et al., Single-band upconversion nanoprobes for multiplexed simultaneous in situ molecular mapping of cancer biomarkers, Nat. Commun. 6 (2015) 6938–6943.
[15] C. Liu, L. Chang, H. Wang, J. Bai, W. Ren, Z. Li, Upconversion nanophosphor: an efficient phosphopeptides-recognizing matrix and luminescence resonance energy transfer donor for robust detection of protein kinase activity, Anal. Chem. 86 (2014) 6095–6102.
[16] G. Jalani, R. Naccache, D.H. Rosenzweig, S. Lerouge, L. Haglund, F. Vetrone, et al., Real-time, non-invasive monitoring of hydrogel degradation using LiYF4:Yb^{3+}/Tm^{3+} NIR-to-NIR upconverting nanoparticles, Nanoscale 7 (2015) 11255–11262.
[17] H. Li, L. Wang, NaYF4:Yb^{3+}/Er^{3+} nanoparticle-based upconversion luminescence resonance energy transfer sensor for mercury(II) quantification, Analyst 138 (2013) 1589–1595.
[18] C. Liu, F. Wang, Y. Wang, Z. Li, A versatile fluorescence turn-on assay for highly sensitive detection of tyrosine phosphatase activity, Chem. Commun. 50 (2014) 13983–13986.
[19] D.G. Didier Casanova, Thierry Gacoin, Jean-Pierre Boilot, Antigoni Alexandrou, Single lanthanide-doped oxide nanoparticles as donors in fluorescence resonance energy transfer experiments, J. Phys. Chem. B 110 (2006) 19264.
[20] T.G. Arnaud Huignard, Jean-Pierre Boilot*, Synthesis and luminescence properties of colloidal YVO4:Eu phosphors, Chem. Mater. 12 (2000) 1090.
[21] X. Peng, X. Xu, D.R. Draney, G.M. Little, J. Chen, W.M. Volcheck, et al., Preparation of Nonfluorescent Near-IR Quencher Cyanine Dyes for Probe Labeling, LI-COR, Inc., USA, 2012, pp. 86.
[22] K. Kiyose, S. Aizawa, E. Sasaki, H. Kojima, K. Hanaoka, T. Terai, et al., Molecular design strategies for near-infrared ratiometric fluorescent probes based on the unique spectral properties of aminocyanines, J. Chem. Eur. 15 (2009) 9191–9200.
[23] T. Myochin, K. Hanaoka, S. Iwaki, T. Ueno, T. Komatsu, T. Terai, et al., Development of a series of near-infrared dark quenchers based on Si-rhodamines and their application to fluorescent probes, J. Am. Chem. Soc. 137 (2015) 4759–4765.
[24] F. Jabeen, M. Najam-ul-Haq, M. Rainer, Y.G. uzel, C.W. Huck, G.K. Bonn, Newly fabricated magnetic lanthanide oxides core–shell nanoparticles in phosphoproteomics, Anal. Chem. 87 (2015) 4726–4732.
[25] X. Zhang, C. Liu, H. Wang, H. Wang, Z. Li, Rare earth ion-Mediated fluorescence accumulation on a single microbead: an ultrasensitive strategy for the detection of protein kinase activity at the single-Cell level, Angew. Chem. Int. Ed. 54 (2015) 15186–15190.

Biographies

Ben Hao Li is a master student in Shaanxi Normal University, China. His current interest focuses on the design and synthesis of innovative sensors

Ya Ling Zhang obtained her Master's degree from the Beijing Institute of Genomics, Chinese Academy of Sciences, China, and now is a Ph.D. candidate in Shaanxi Normal University, China. Her current interest is centered on the design, bioactive evaluation and molecular mechanism research of new compounds, and fluorescence based sensors, nanosensors, and functional materials.

Fan Shi Li is a master student in Northwest University, China. His current research interests focuses on a new technology for detecting of tyrosine kinase inhibitors.

Wei Wang works as a chemistry associate professor in the School of Chemistry & Chemical Engineering, Shaanxi Normal University, China. Her current research interests focuses on medicinal chemistry and synthetic chemistry.

Juan Liu is a master student in Shannxi Normal University, China. Her current research focuses on the design and synthesis of antitumor drug.

Min Liu is a master student in Shaanxi Normal University, China. Her current research focuses on the synthesis of drug.

Yi Cui is a master student in Shaanxi Normal University, China. His current interest is the design and synthesis of SGLT2 inhibitor.

Xia Bing Li obtained a BA in Chemistry from Shaanxi Normal University in 2010, followed by a PhD in Organic Chemistry from the University of Sheffield in 2014. She is currently a lecture in the School of Chemistry & Chemical Engineering, Shaanxi Normal University. Her current research interests focuses on the development of synthetic methodology with organometallic compounds.

Bao Lin Li works as a chemistry professor in the School of Chemistry & Chemical Engineering, Shaanxi Normal University, China. His current research interests focuses on medicinal chemistry and synthetic chemistry.